



Pyrochlore-group minerals from the Loe-Shilman Carbonatite Complex, NW Pakistan: implications for evolution of carbonatite system

Asad Khan^{1,2,*}, Shah Faisal², Zaheen Ullah³, Liaqat Ali², Abuzar Ghaffari¹, Javed Nawab⁴, Mehboob Ur Rashid⁵

¹ Department of Geology, FATA University, FR Kohat 26100, KP, Pakistan

² National Centre of Excellence in Geology, University of Peshawar, Peshawar 25130, KP, Pakistan

³ Key Laboratory of Metallogenic Prediction of Nonferrous Metals and Geological Environment Monitoring, Ministry of Education, School of Geosciences and Info-Physics, Central South University, Changsha 410083, China

⁴ Department of Environmental Sciences, Abdul Wali Khan University, Mardan, Pakistan

⁵ Geoscience Advance Research Laboratories Islamabad, Geological Survey of Pakistan, Pakistan

ARTICLE INFO

Submitted: December 2020

Accepted: February 2021

Available on line: April 2021

* Corresponding author:
asadgeo89@gmail.com

Doi: 10.13133/2239-1002/17360

How to cite this article:
Khan A. et al. (2021)
Period. Mineral. 90, 277-287

ABSTRACT

This study reports new occurrence of niobium mineralization from the Loe-Shilman carbonatite complex, NW Pakistan. The complex is predominantly comprised of calcite carbonatite, intruded by dolomite carbonatite, and minor late-stage carbonatite veins, intruding the earlier two varieties. Pyrochlore group minerals, which are the major Nb phases in the carbonatites and overlying supergene laterite, manifest numerous textural and compositional discrepancies. Pyrochlores observed in calcite and dolomite carbonatites of the complex are typified by oscillatory zoning, and are compositionally Ca-Na-pyrochlore, and therefore, illustrating crystallization under primary magmatic conditions. However, relatively Ta poor (2.42-5.11 wt%) and Nb rich (60.04-62.14 wt%) pyrochlores preserved in dolomite carbonatite are reflecting a more evolved nature of the dolomite carbonatite compared to Ta rich (6.89-10.11 wt%) pyrochlore of the calcite carbonatite. In addition, pyrochlores of the late-stage carbonatite veins record patchy zonation and are characterized by A-site vacancies, likely due to leaching of Na and Ca, and enrichment of Ba-REE-Sr during hydrothermal alteration by a relatively low pH, Na and/or Si poor fluids. Similarly, intensively patchy zoned, porous and Fe³⁺ bearing A-site deficient bariopyrochlore in supergene laterite are produced by complete leaching of Ca and Na from A-site, and by partial replacement of strongly-bounded Nb at B-site by Fe³⁺ during supergene conditions.

Keywords: Northwest Pakistan; Loe-Shilman carbonatite; pyrochlore; compositional and textural variations; magmatic and hydrothermal processes; deposit evolution.

INTRODUCTION

Niobium is designated as a strategic or critical refractory metal, which has several high-tech industrial uses such as manufacturing of high-strength low-alloys steel, corrosion and heat resistant alloys, variety of superconductors, high performance batteries and magnets (Chakmouradian et al., 2015; Chebotarev et al., 2017; Mitchell et al.,

2020). Although Nb has numerous high-tech industrial applications, which has increased its global production by four times since 2000 (Chebotarev et al., 2017; Mitchell et al., 2020), however, there are few limited exploitable deposits of Nb in the world. The largest Nb production in the world comes from three major operating mines, i.e., Araxá and Catalão-II, in Brazil, and St. Honoré, in Canada



(~92% and 7% of global production, respectively); (Cordeiro et al., 2011; Mitchell et al., 2020). Due to the increasing demand in high-tech, and as an important economic interest metal, many countries are focused on exploring new resources of Nb indigenously.

The bulk of commercial Nb comes from pyrochlore group minerals which commonly occur in economically viable amounts in carbonatites and their weathering products (Chakhmouradian and Williams, 2004; Chakhmouradian et al., 2015). Pyrochlore group minerals show significant structural and compositional variations due to exchange reactions during the process of evolution of carbonatite complexes (Nasraoui and Bilal, 2000; Cordeiro et al., 2011; Chebotarev et al., 2017; Khromova et al., 2017; Walter et al., 2018). This study describes new occurrence of pyrochlore mineralization from the Loe-Shilman carbonatite complex in NW Pakistan, and is focused on to delineate the chemical composition of pyrochlore group minerals found in various carbonatite bodies and in its overlying supergene laterite deposits of the complex. Main focus of the present data and interpretation are to characterize pyrochlore composition, and better compute their geochemical evolution in carbonatite system of the Loe-Shilman carbonatite complex, NW Pakistan.

GEOLOGICAL AND MINERALOGICAL DESCRIPTION

The Loe-Shilman carbonatite complex is located in the Khyber district, in the vicinity of Pakistan and Afghanistan border (Figure 1a). Along with the Sillai Pattai, Koga and Jambil carbonatites, and the Warsak, Shewa-Shahbazgarhi and Ambela granitic complexes, it is combined into the Peshawar Plain Alkaline Igneous Province (Figure 1a); (Kempe and Jan, 1970, 1980; Butt, 1981; Jan et al., 1981; Ahmad et al., 2013). The Loe-Shilman complex is an East-West trending sill-like intrusion that separate Precambrian slates and phyllites in the south from Paleozoic schists, and metasedimentary dolomite in the north (Figure 1b). The complex is ~2.5 km long, and ~170 m wide in its central part (Jan et al., 1981). The complex has yielded K-Ar phlogopite age of 31 ± 2 Ma (Le Bas et al., 1987) and apatite fission track age of 30 ± 1.54 Ma (Khattak et al., 2008). However, the first author of this article has recently documented a U-Pb zircon crystallization age of 90.6 ± 1.0 Ma (MSWD=1.6, n=33) (Khan, 2021). Moreover, the complex can be divided into calcite and dolomite carbonatites, and minor late-stage carbonatite veins (Figures 1b, 2a). Detailed petrographic descriptions of the Loe-Shilman carbonatite complex are already given by Jan et al. (1981). These are briefly summarized here and we present various textural characteristics of the pyrochlore-group minerals, as these are the focus of this study.

Calcite carbonatite

The calcite carbonatite is the most extensive carbonatite intrusion of the complex. It is white on fresh surface, and pale to dark brown on weathered surface. The calcite carbonatite is dominated by calcite (60-70%), and contain variable amounts of fluorapatite (10-15%), biotite (10-15%), amphiboles (8-12%), magnetite (2-4%), pyrochlore (1-3%), zircon (~1%) and monazite (<1%); (Figure 2 b,c). Calcites occur as equigranular and euhedral to subhedral coarse grains, whereas amphiboles (magnesian-arfvedsonit and richterite) occur as long pleochroic prisms. Rounded or prismatic crystals of fluorapatite observed embedded in calcite matrix (Figure 2 b,c). Large flakes of biotite present are sometimes oriented and deformed. Pyrochlores exist as dark brown to black, and irregularly disseminated octahedral crystals. Generally, pyrochlores are 2mm to 1cm long euhedral crystals, and typically show oscillatory zoning pattern without any resorbed pyrochlore cores (Figure 3a). Pyrochlores contain inclusions of calcite and fluorapatite and in some cases reflect intergrowth texture with calcite and fluorapatite (Figure 2f). The association of pyrochlores with calcite and fluorapatite, and lack of resorbed pyrochlore cores indicate in-situ crystallization of pyrochlores in the calcite carbonatite of the complex.

Dolomite carbonatite

The dolomite carbonatite either intrude the calcite carbonatite or occur along the southern contact of calcite carbonatite and host rocks (Figure 1b). The dolomite carbonatite is predominantly comprised of medium to coarse grained, subhedral dolomite (>75%), and magnetite (5-10%), ovoid and prismatic fluorapatite (5-10%), euhedral pyrochlore (1-3%), minor acicular amphibole (magnesian-arfvedsonit and richterite), and traces of biotite (Figure 2d). Pyrochlores in the dolomite carbonatite are relatively fine grained; however, their textural characteristics are similar to the calcite carbonatite (Figure 3b).

Late-stage carbonatite veins

The late-stage carbonatitic veins are intruding the calcite and dolomite carbonatites and are comprised of calcite (60-70%), dolomite (12-16%), barite (8-15%), biotite (<10%), monazite (up to 4%), and pyrochlore (1-2%); (Figure 2e). Fluorapatite is mainly missing in these carbonatitic veins. Pyrochlores in the late-stage carbonatite veins occur as anhedral to euhedral, fine grained disseminated crystals or aggregates (Figure 2e). These pyrochlores show patchy zonation that overprints the primary magmatic oscillatory zoning (Figure 3c). The patchy overprinting observed starting at the grain margin, whereby an alteration front moves towards the centre of the pyrochlore (Figure 3c).

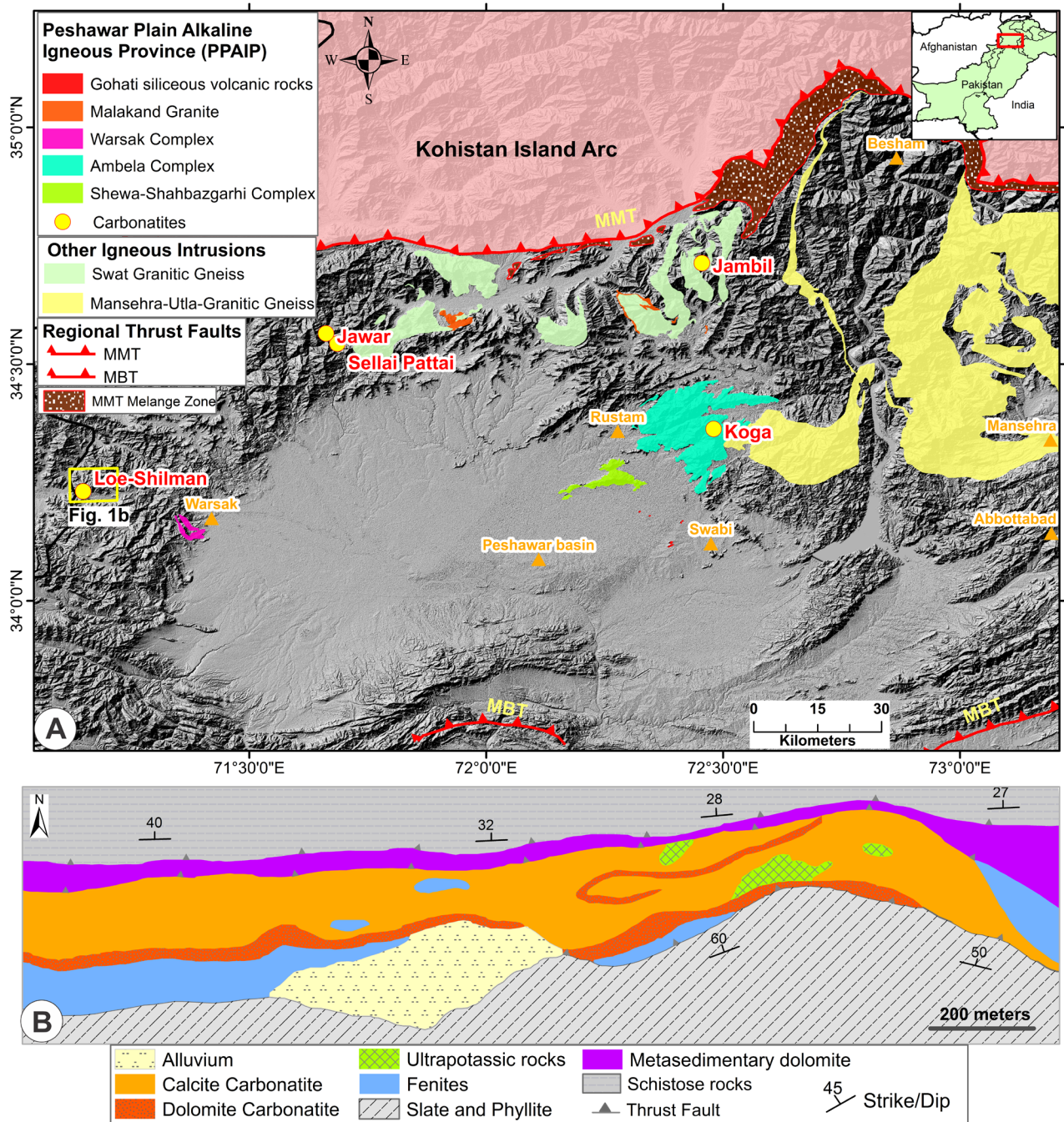


Figure 1. a) Map showing distribution of alkaline rocks and carbonatites of the PPAIP between MMT and MBT; b) Geological map of the Loe-Shilman carbonatite complex (Modified after Jan et al., 1981).

Supergene laterite

Intensive lateritic weathering of the bed rock carbonatites of the Loe-Shilman complex under humid-subtropical to tropical climatic conditions has developed a supergene laterite layer of variable thickness over the carbonatite complex. The supergene lateritic layer consists of dark

brown ochres with relicts of carbonatite, and contains goethite, kaolinite, zircon, pyrochlores, monazite and rutile minerals. Pyrochlore grains found in the supergene laterite are highly porous with intense patchy zonation and vestige of oscillatory zoning (Figure 3d).

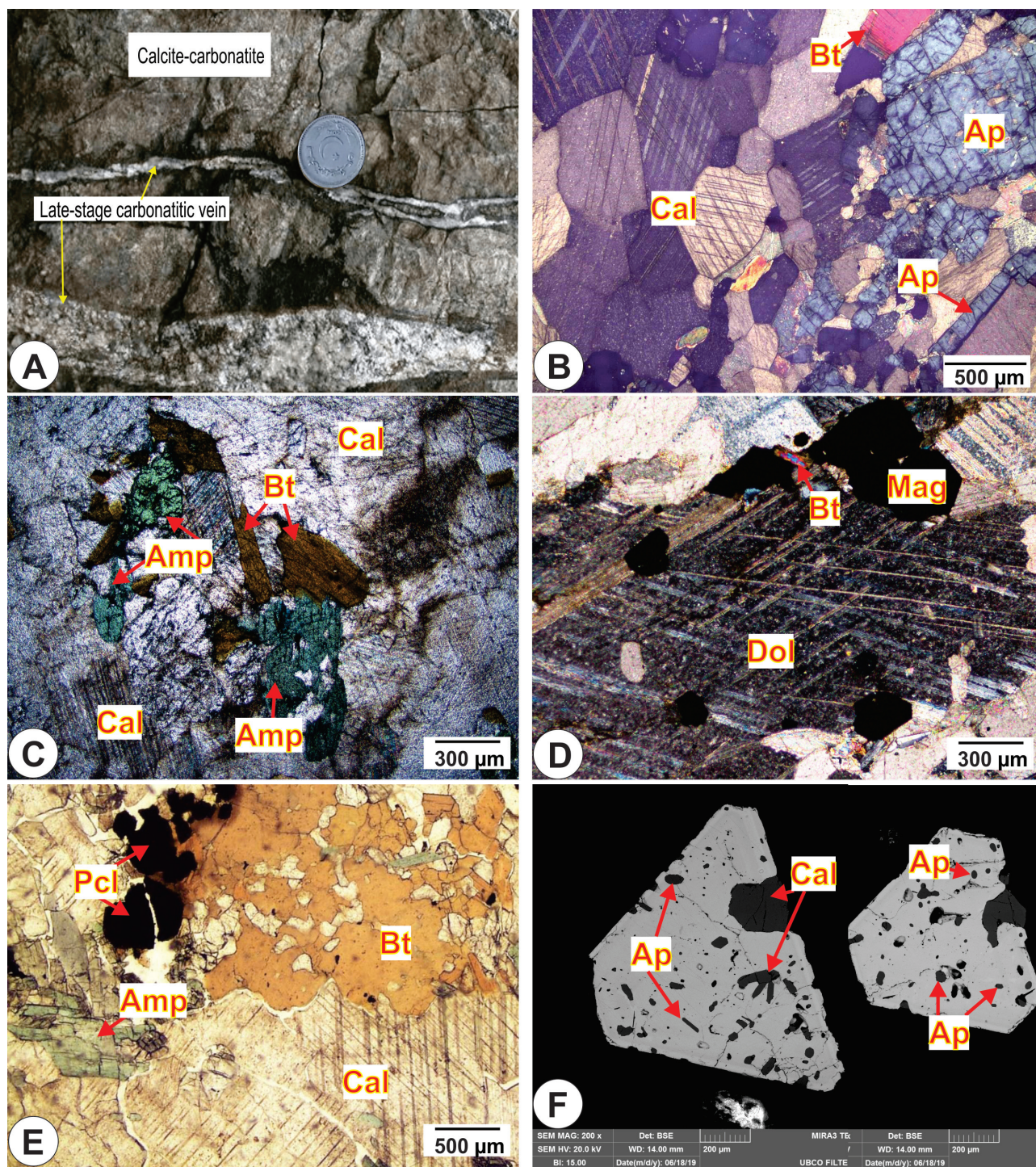


Figure 2. a) Outcrop picture of late-stage carbonatite veins cutting calcite carbonatite; b,c) photomicrographs of calcite carbonatite comprised of equigranular and subhedral calcite (Cal), subhedral to euhedral apatite (Ap), flakes of biotite (Bt), and amphibole (Amp); d) photomicrographs of dolomite carbonatite comprised of predominantly dolomite (Dol), subordinate subhedral to euhedral magnetite (Mag) and Bt; e) photomicrographs of hydrothermal carbonatite vein comprised of Cal, Bt, Amp and pyrochlore (Pcl); f) back scattered electron image of Pcl containing inclusions of Ap and Cal.

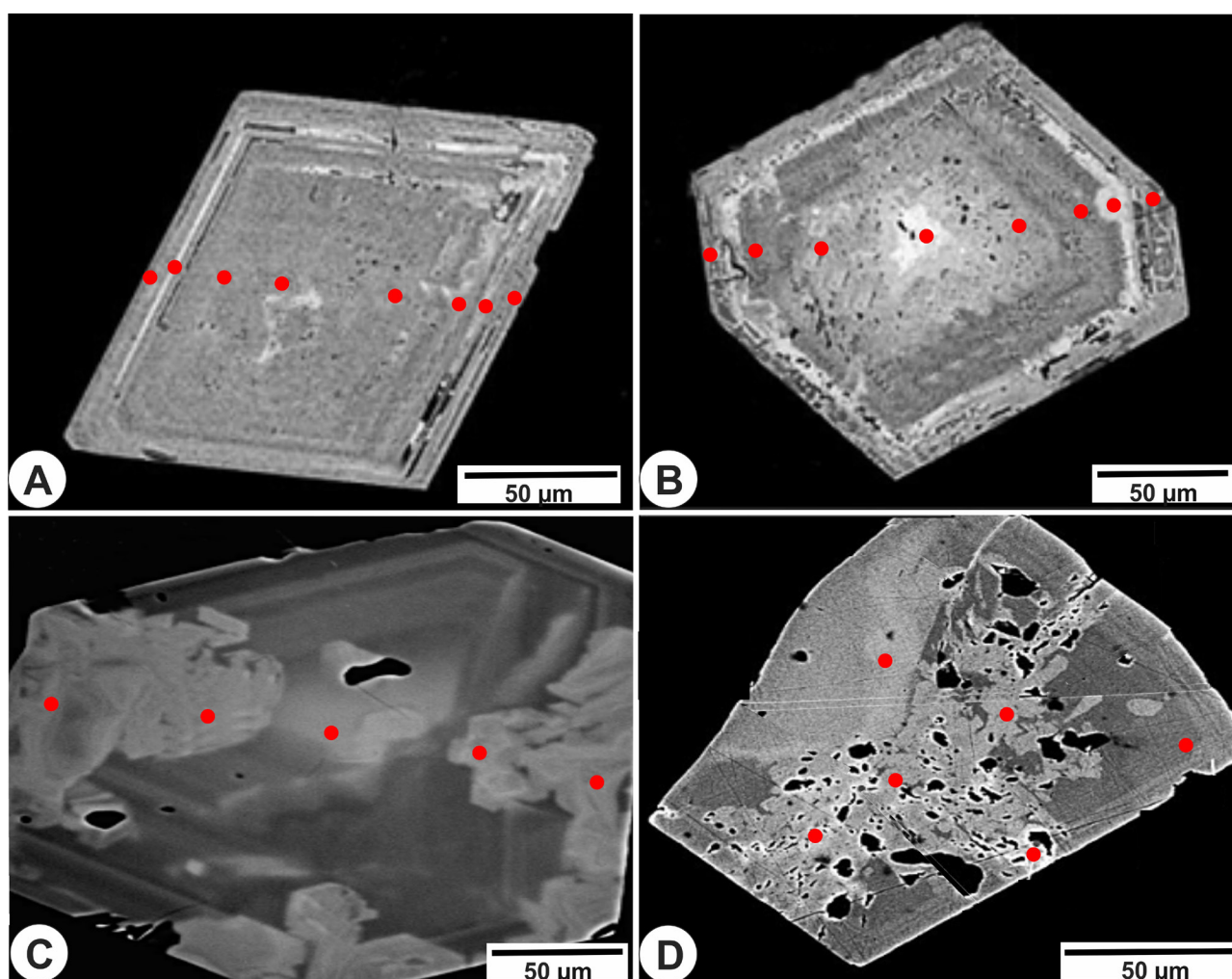


Figure 3. Back scattered electron image of oscillatory zoned pyrochlore crystals in calcite and dolomite carbonatites (a,b) patchy zoned pyrochlore overprinting primary oscillatory zoning occurring in late-stage carbonatite vein (c) and patchy zoned, porous pyrochlore in supergene laterite (d).

PYROCHLORE COMPOSITION

Pyrochlore grains collected from various carbonatites and supergene laterite were mounted in epoxy resin, and were then polished to expose equatorial sections. Polished grain mounts were examined to observe zoning patterns of the pyrochlore-group minerals through scanning electron microscopy in Back-scattered electron (BSE) mode at the University of British Columbia (UBC), Canada. During analysis the scanning electron microscope was operated at an accelerating voltage of 20 kV, a beam current of 1 nA, and a count time of 50 s. The BSE images were subsequently used for choosing analytical points to determine the chemical composition of the pyrochlores through Laser Ablation-Inductively Coupled Plasma-Mass Spectrometry (LA-ICP-MS) at the Fipke Laboratory for Trace Element Research facility housed at

the UBC, Canada. The LA-ICP-MS setup is comprised of a Photon Machines Analyte 193 Excimer laser coupled to an Agilent 8900 triple quadrupole ICP-MS. Helium (0.7 L/min) was used as the ablation cell carrier gas, and was mixed with Argon (0.9 L/min) before the plasma using an in-house glass mixing valve that also served as a signal smoothing device. The instrument was optimized before each analytical run using the Standard Reference Material NIST610 for maximum signal coupled with maintaining oxide and doubly charged ion ratios below 1% of the certified value. Target domains were ablated with a laser spot size of 50 μm at the repetition rate of 8 Hz, and a fluence of 5 J/cm². Trace element data were normalized to NIST 610 using ⁴³Ca as the internal standard with NIST 612 and BCR-2G serving as secondary check standards. All data were processed using Iolite v4 (Paton

et al., 2011).

The general formula of pyrochlore super-group is $A_{2-m}B_2X_{6-w}Y_{1-n} \cdot pH_2O$ (Hogarth, 1977; Atencio et al., 2010). The A-site is typically occupied by large cations such as As, Ba, Bi, Ca, Cs, K, Mg, Mn, Na, Pb, REE, Sb, Sr, Th, U and Y. The B-site normally accommodate highly charged smaller cations such as Nb, Ta, Ti, Zr, Fe^{3+} , Al, Si and W^{+5} (Zurevinski and Mitchell, 2004; Caprilli et al., 2006). The Y and X are anions and filled with O, OH and F. The A and Y sites can be either partially or fully vacant (Lumpkin and Ewing, 1995; Wall et al., 1996). The structural formulae of the analyzed pyrochlores from the Loe-Shilman complex have been calculated on the basis of 2 B-site cations which classify the Loe-Shilman pyrochlore within the pyrochlore group (Figure 4a).

Pyrochlore-group minerals are the principal Nb phases observed in the Loe-Shilman carbonatite complex. Representative compositions of pyrochlore-group minerals are presented in Table 1. In general, the Nb_2O_5 contents of the all analyzed pyrochlore are high (55.25-62.14 wt%), while the concentrations of radioactive elements are low i.e. ThO_2 concentration varies from 0.19 to 1.37 wt% and UO_2 from 0.14 to 1.75 wt% (Table 1). Like the radioactive elements the total REE+Y concentrations are also low ($Y+REE_2O_3=1.75-3.86$ wt%) in the calcite and dolomite carbonatites, but may reach up to 4.16-9.41 wt% in the pyrochlore occurring in late-stage carbonatite veins and supergene laterite (Table 1).

Oscillatory zoning patterns of pyrochlore crystals in calcite and dolomite carbonatites are indistinguishable but there are compositional variations in pyrochlores from the two carbonatite types. The chemical data also

show that none of the pyrochlore-subgroups which are found in the calcite carbonatite occur in the dolomite carbonatite, except the core of a few larger pyrochlore crystals in dolomite carbonatites, which show similarity to pyrochlore composition in calcite carbonatites. Pyrochlores in the dolomite carbonatites are relatively rich in Nb_2O_5 (60.04-62.14 wt%), TiO_2 (4.35-5.21 wt%), BaO (1.45-2.30 wt%) and SrO (1.79-2.69 wt%), but low in Ta_2O_5 (2.12-5.11 wt%) with similar contents of CaO, Na_2O , UO_2 , ThO_2 , ZrO_2 and REE oxides as in calcite carbonatites (Table 1). In calcite and dolomite carbonatites, pyrochlores with vacancies at A-site are absent, and are Ca-Na-pyrochlores in composition (Figure 4b). However, the overprinting patchy zones in pyrochlores found in late-stage carbonatite veins and supergene laterite are predominantly A-site vacant Ba-REE-Sr rich pyrochlore and bariopyrochlore. Moreover, the proportions of A-site vacancies and Ba content increase from late-stage carbonatitic veins to supergene laterite pyrochlore (Figure 4b, Table 1). The overprinting patchy zones are characterized by lower Nb_2O_5 (<59.1 wt%), Ta_2O_5 (<2.15 wt%), CaO (<5.62 wt%), Na_2O (<1.13 wt%), and higher BaO (up to 13.42 wt%), SrO (up to 4.16 wt%), and REE oxides compared to oscillatory zoned areas, which resemble either the composition of oscillatory zoned pyrochlores in calcite or dolomite carbonatites (Table 1). Moreover, pyrochlores in supergene laterite contain Fe_2O_3 from 1.1-4.2 wt%.

INTERPRETATION AND DISCUSSION

The Loe-Shilman carbonatite complex: A potential Nb deposit

In general, the contents of Nb_2O_5 in pyrochlore crystals

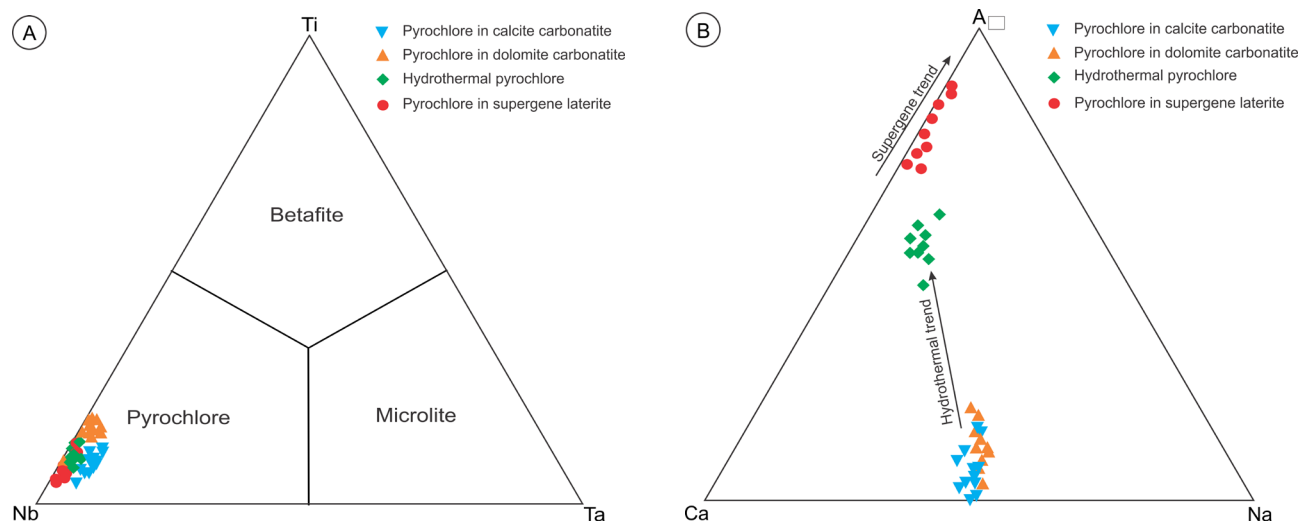


Figure 4. (a) Classification diagram of pyrochlore-group minerals from the Loe-Shilman carbonatite complex (after Hogarth, 1977) and (b) ternary plots of Ca, Na and A-site vacancy showing the hydrothermal and supergene trends of the pyrochlores.

Table 1. Representative compositions of the pyrochlore-group minerals from the Loe-Shilman carbonatite complex.

Wt%	Pyrochlore in calcite carbonatite					Pyrochlore in dolomite carbonatite					Hydrothermal pyrochlore			Pyrochlore in supergene laterite						
	61.71	59.26	57.76	59.93	56.12	55.48	60.12	61.24	60.39	61.15	62.14	60.04	55.88	56.65	55.25	57.94	59.07	58.19		
Nb ₂ O ₅	7.21	9.13	10.11	7.34	9.93	10.1	8.16	6.89	3.31	5.11	3.07	2.42	4.61	1.06	1.48	2.15	1.2	1.48	1.39	
Ta ₂ O ₅	-	-	0.12	-	0.11	0.23	0.12	-	0.04	0.6	-	-	-	0.26	-	0.2	-	0.31	-	
SiO ₂	3.11	2.64	2.39	1.15	3.15	2.16	1.67	1.91	4.71	4.35	5.21	5.14	5.04	3.13	2.81	2.2	3.24	1.26	1.97	
TiO ₂	0.17	1.05	0.9	1.11	0.33	0.91	0.26	1.17	0.65	0.53	0.09	0.32	0.36	0.42	1.77	0.69	1.6	0.62	0.91	
ZrO ₂	0.36	-	-	1.02	0.59	0.85	0.19	0.14	-	-	0.56	-	0.71	1.17	1.75	1.12	1.6	1.6	1.21	
UO ₂	1.01	1.12	1.2	0.85	1.09	1.09	1.15	1.12	1.13	1.2	0.78	0.19	1.12	1.28	1.37	1.25	1.26	1.26	1.03	
ThO ₂	0.21	-	-	-	0.79	0.21	0.11	0.45	-	-	0.32	-	-	-	-	-	1.1	2.1	4.2	
Fe ₂ O ₃	0.44	0.57	0.43	0.55	0.32	0.25	0.34	0.45	0.46	0.53	0.2	0.32	0.47	1.8	0.36	0.78	0.56	0.43	0.47	
Y ₂ O ₃	1.1	0.39	0.61	0.62	0.96	0.69	0.87	0.79	0.68	0.71	0.35	0.67	0.61	1.7	1.3	1.6	0.71	0.67	0.58	
La ₂ O ₃	1.2	0.79	0.85	1.21	2.12	2.92	2.09	2.14	2	2.12	2.14	1.73	2.05	4.03	6.05	5.62	2.14	3.99	2.98	
Ce ₂ O ₃	-	-	-	-	-	-	-	-	-	-	-	-	-	1.5	1.7	0.39	0.75	0.39	0.25	
Nd ₂ O ₃	-	-	-	-	-	-	-	-	-	-	0.16	-	0.13	0.07	0.23	0.02	0.39	0.14	0.33	
MnO	11.97	12.01	12.98	13.14	12.76	12.98	13.12	13.11	12.74	11.86	11.61	12.39	11.41	5.62	4.48	5.29	3.82	3.45	4.27	
CaO	0.35	0.23	0.23	0.27	0.89	0.67	0.13	0.19	1.89	1.45	2.3	2.18	2.17	5.29	7.23	9.09	9.12	11.89	13.42	
BaO	1.13	0.69	0.35	0.48	0.95	0.48	1.41	1.19	1.79	2.35	2.69	2.61	2.15	3.7	4.16	4.02	2.9	2.43	3.24	
SrO	6.51	6.73	7.12	7.07	6.71	7.02	6.76	6.94	6.99	6.33	6.89	6.98	6.75	1.11	1.13	0.89	0.3	0.5	0.03	
Na ₂ O	96.48	94.38	95.05	94.26	96.82	96.04	93.64	96.42	97.63	97.53	97.52	97.09	97.62	88.02	92.47	90.56	88.63	91.59	94.47	
Total																				
Atoms per formula unite calculated on basis of 2 B-site cations																				
Nb	1.720	1.686	1.673	1.777	1.621	1.656	1.744	1.731	1.705	1.664	1.692	1.714	1.677	1.781	1.767	1.800	1.714	1.766	1.656	
Ta	0.121	0.156	0.176	0.131	0.173	0.181	0.149	0.119	0.055	0.085	0.051	0.040	0.077	0.020	0.028	0.042	0.021	0.027	0.024	
Ti	0.144	0.125	0.115	0.057	0.151	0.107	0.085	0.091	0.218	0.199	0.240	0.236	0.234	0.166	0.146	0.119	0.159	0.063	0.093	
Zr	0.005	0.032	0.028	0.035	0.010	0.029	0.009	0.036	0.020	0.016	0.003	0.010	0.011	0.014	0.060	0.024	0.051	0.020	0.028	
Fe ³⁺	0.010	0.000	0.000	0.000	0.038	0.010	0.006	0.022	0.000	0.000	0.015	0.000	0.000	0.000	0.000	0.000	0.054	0.104	0.199	
Si	0.000	0.000	0.008	0.000	0.007	0.015	0.008	0.000	0.002	0.037	0.000	0.000	0.000	0.018	0.000	0.014	0.000	0.020	0.000	
Sum B-site	2.000	2.000	2.000	2.000	2.000	2.000	2.000	2.000	2.000	2.000	2.000	2.000	2.000	2.000	2.000	2.000	2.000	2.000	2.000	

Table 1. ... Continued

Wt%	Pyrochlore in calcite carbonatite					Pyrochlore in dolomite carbonatite					Hydrothermal pyrochlore			Pyrochlore in superegene laterite					
Ca	0.791	0.810	0.891	0.923	0.873	0.918	0.947	0.895	0.840	0.774	0.761	0.810	0.755	0.424	0.331	0.408	0.268	0.244	0.288
Mn	0.000	0.000	0.000	0.000	0.000	0.000	0.000	0.000	0.000	0.000	0.008	0.000	0.007	0.004	0.013	0.001	0.022	0.008	0.018
Ba	0.008	0.000	0.006	0.000	0.022	0.017	0.003	0.000	0.046	0.035	0.055	0.052	0.053	0.146	0.195	0.257	0.234	0.308	0.331
Sr	0.040	0.025	0.013	0.010	0.035	0.018	0.055	0.044	0.064	0.083	0.095	0.092	0.077	0.151	0.166	0.168	0.110	0.093	0.118
Na	0.778	0.821	0.884	0.899	0.831	0.899	0.883	0.857	0.834	0.748	0.817	0.826	0.809	0.152	0.151	0.124	0.038	0.064	0.004
Y	0.014	0.019	0.015	0.019	0.011	0.009	0.012	0.015	0.015	0.017	0.007	0.010	0.015	0.068	0.013	0.030	0.020	0.015	0.016
LREE	0.052	0.027	0.034	0.044	0.072	0.087	0.073	0.068	0.061	0.063	0.056	0.054	0.060	0.186	0.228	0.201	0.086	0.122	0.088
U	0.005	0.000	0.000	0.015	0.008	0.012	0.003	0.002	0.000	0.000	0.008	0.000	0.010	0.018	0.027	0.018	0.023	0.024	0.017
Th	0.014	0.016	0.017	0.013	0.016	0.016	0.018	0.016	0.016	0.017	0.011	0.003	0.016	0.021	0.022	0.020	0.019	0.019	0.015
Sum A-site	1.703	1.719	1.861	1.923	1.869	1.978	1.994	1.898	1.876	1.737	1.818	1.847	1.802	1.170	1.147	1.228	0.819	0.897	0.894
A-deficit	0.297	0.281	0.139	0.077	0.131	0.022	0.006	0.102	0.124	0.263	0.182	0.153	0.198	0.850	0.853	0.772	1.181	1.103	1.106
Vacancy %	14.8	14.0	7.0	3.8	6.5	1.1	0.3	5.1	6.2	13.2	9.1	7.6	9.9	41.5	42.7	38.6	59.1	55.1	55.3
Pyrochlore	86.65	85.71	85.17	90.45	83.35	85.16	88.17	89.14	86.17	85.42	85.33	86.13	84.33	90.53	91.06	91.77	90.46	95.19	93.40
Microcline	6.09	7.94	8.97	6.66	8.87	9.33	7.56	6.15	2.80	4.35	2.58	2.02	3.89	1.03	1.43	2.15	1.13	1.43	1.34
Betafite	7.26	6.35	5.86	2.89	7.78	5.52	4.28	4.71	11.02	10.23	12.09	11.85	11.78	8.44	7.51	6.08	8.41	3.38	5.26

from the Loe-Shilman carbonatite complex is high (55.25–62.14 wt%), whereas, Ta₂O₅ and TiO₂ vary from 1.06 to 10.11 wt% and 1.15 to 5.21 wt%, respectively (Table 1). Therefore, the high atomic proportions of Nb (1.62–1.80 apfu) compared to Ta (0.02–0.18 apfu) and Ti (0.06–0.24 apfu) at B-site classify the Loe-Shilman pyrochlore-group minerals as pyrochlore *sensu stricto* (Figure 4a). The Nb concentration of the Loe-Shilman pyrochlore is high enough to designate the Loe-Shilman carbonatites potential for Nb exploitation. Moreover, the concentrations of radioactive elements are low i.e., ThO₂ concentration varies from 0.19 to 1.37 wt% and UO₂ from 0.14 to 1.75 wt% (Table 1). Highly radioactive pyrochlore are reported from the Sokli phosphorite-carbonatite complex, Finland (UO₂=0.05–21 wt% and ThO₂=0.16–5.22 wt%; (Lee et al., 2006) and Latium, Italy (UO₂=14.74–33.68 wt% and ThO₂=0.44–2.84 wt%; Caprilli et al., 2006). Exploitation of such a high radioactive pyrochlore could give rise to environmental pollution by dispersion of radioactive elements in the ecosystem of an area. However, the Loe-Shilman pyrochlores are similar in composition to the non-radioactive pyrochlore of the Panda Hill carbonatite deposit in Tanzania (Boniface, 2017). The low concentration of radioactive elements in the Loe-Shilman pyrochlore points to environmental friendly exploitation of Nb in the Loe-Shilman area. Whereas, the low REE+Y contents of pyrochlore in calcite and dolomite carbonatites (1.75–3.86 wt%), which cover most of the outcrop area of the Loe-Shilman complex, indicate unpromising potential for REE+Y.

Chemical evolution of pyrochlore

Oscillatory zoning in pyrochlores found in the calcite and dolomite carbonatite is a typical magmatic feature (Hogarth et al., 2000; Walter et al., 2018). In the calcite and dolomite carbonatites, pyrochlore and apatite coexist, which may reflect that at initial stages of carbonatite magmatism Nb and Ta are transported as phosphate and fluorine complexes (Knudsen, 1989; Hogarth et al., 2000; Cordeiro et al., 2011). Due to relatively high solubility of Nb than Ta in carbonatitic magma, Nb-rich pyrochlore occur in a more evolved magma and relatively Nb-poor and Ta-rich pyrochlore in primitive magma (Knudsen, 1989; Cordeiro et al., 2011). Similarly, pyrochlore progressively evolve into Na-Ca-Nb enriched and Ta-Th-U-REE depleted composition in carbonatitic magma (Hogarth et al., 2000; Lee et al., 2006). In Kola carbonatite complex, Th-Ca-Na dominant pyrochlore evolves towards Ba-Sr rich pyrochlores (Chakhmouradian and Williams, 2004). Oscillatory zoned pyrochlore in the magmatic calcite and dolomite carbonatites of the Loe-Shilman complex indicates similar trends but early formed Ta enriched pyrochlore are Th and U poor. Ta-

rich pyrochlores in calcite carbonatite can be interpreted as less evolved (primitive) phases and relatively Ta poor, and Nb rich pyrochlores in dolomite carbonatite as more evolved phases (Cordeiro et al., 2011).

Pyrochlores characterized by patchy zonation which overprint primary magmatic oscillatory zoning in late-stage carbonatite veins and supergene laterite are typical of hydrothermal and supergene alterations of pre-existing pyrochlores derived either from calcite or dolomite carbonatites (Lumpkin and Ewing, 1995; Wall et al., 1996; Nasraoui and Bilal, 2000; Chebotarev et al., 2017; Walter et al., 2018). The patchy zones in pyrochlores found in late-stage carbonatite veins in the Loe-Shilman complex are characterized by A-site vacancies, enrichment of Ba-REE-Sr and strong depletion of Na with moderate loss of Ca (Figure 4b). The A-site vacancies and enrichment of Ba increase in addition to complete loss of Na and almost complete loss of Ca in patchy zoned pyrochlores in supergene laterite of the Loe-Shilman complex (Figure 4b). The trend from Ca-Na-pyrochlores in calcite and dolomite carbonatites towards A-site deficient Ba-REE-Sr rich pyrochlore and bariopyrochlore in late stage carbonatite veins and supergene laterite is linked with substitution of Ba-REE-Sr with Ca and Na, and subsequent vacancies at the A-site (Nasraoui and Bilal, 2000; Cordeiro et al., 2011; Chebotarev et al., 2017; Walter et al., 2018; Figure 4b). Similar trends are described from pyrochlores in the Kola carbonatite, Russia (Chakhmouradian and Williams, 2004) and Sokli carbonatite, Finland (Lee et al., 2006) attributed to supergene or low temperature hydrothermal alteration, and from pyrochlores in the Bingo and Lueshe carbonatites, Congo (Williams et al., 1997; Nasraoui and Bilal, 2000, respectively), as a result of surficial weathering. Moreover, presences of Fe₂O₃ in patchy zoned pyrochlores in supergene laterite indicate replacement of strongly-bounded Nb at B-site by Fe³⁺ by supergene fluids.

The late-stage veined carbonatites are devoid of apatite and contain abundant monazite compared to other carbonatites of the Loe-Shilman complex. The abundance of monazite crystallization may be at the expense of complete dissolution of apatite. The cation-substitution in pyrochlore is described to occur at relatively acidic conditions (Nasraoui and Bilal, 2000). The low pH conditions are probably responsible for total dissolution of apatite in late-stage carbonatite veins that led to the lack of apatite in the late-stage carbonatite veins. The crystallization of monazite at absence of apatite also suggests an acidic, Na and/or Si poor nature of hydrothermal fluids responsible for apatite dissolution (Harlov and Förster, 2003; Harlov et al., 2005), and the most evolved character of the late-stage carbonatite veins (Zirner et al., 2015; Chebotarev et al., 2017).

CONCLUSIONS

Pyrochlore group minerals are the principle Nb phases with low contents of radioactive and REE in the Loe-Shilman carbonatites and overlying supergene laterite. The morphology and compositional variations in pyrochlore-group minerals found in calcite-dolomite- and veined late-stage carbonatites describe the evolution of the Loe-Shilman carbonatite complex, and interaction of primary magmatic carbonatites with hydrothermal fluids. Oscillatory zoned Ca-Na-pyrochlors found in the calcite, and dolomite carbonatites describe primary magmatic character of the carbonatites. However, relatively Ta poor, Nb rich pyrochlors in dolomite carbonatite compared to Ta rich pyrochlors in calcite carbonatite indicate a more evolved nature of the dolomite carbonatite and relatively primate nature of calcite carbonatites. Oscillatory zoned, primary magmatic Ca-Na-pyrochlors evolve towards patchy zoned, cracked, Ba-REE-Sr rich pyrochlors in late-stage hydrothermal veined carbonatites. The elemental redistribution and patchy zonation in hydrothermal pyrochlors possibly caused by acidic, Na and/or Si poor hydrothermal fluids. The porous, patchy zoned, iron bearing briopyrochlors in supergene laterite indicate complete leaching of Ca and Na from A-site and replacement/remobilization of Nb with Fe^{3+} at B-site by supergene fluids. In conclusion, pyrochlore of the Loe-Shilman complex can be an appropriate economic source of Nb with a very low environmental impact due to its minor radioactive nature.

ACKNOWLEDGMENTS

We acknowledge logistic and financial support from the National Centre of Excellence in Geology, University of Peshawar, Pakistan. We also appreciate analytical support provided by the Fipke Laboratory for Trace Element Research (FiLTER), University of British Columbia, Okanagan campus, Canada. The editor and anonymous reviewers are appreciated for their valuable suggestions and comments which certainly improved the manuscript.

REFERENCES

- Ahmad I., Khan S., Lapen T., Burke K., Jehan N., 2013. Isotopic ages for alkaline igneous rocks, including a 26Ma ignimbrite, from the Peshawar plain of northern Pakistan and their tectonic implications. *Journal of Asian Earth Sciences* 62, 414-424.
- Atencio D., Andrade M.B., Christy A.G., Gieré R., Kartashov P.M., 2010. The pyrochlore supergroup of minerals: nomenclature. *The Canadian Mineralogist* 48, 673-698.
- Boniface N., 2017. Crystal chemistry of pyrochlore from the Mesozoic Panda Hill carbonatite deposit, western Tanzania. *Journal of African Earth Sciences* 126, 33-44.
- Butt K.A., 1981. Pyrochlore Group Minerals In Carbonatites From Loe-Shilman, Khyber Agency, NWFP. *Geological Bulletin, University of Peshawar* 14, 111.
- Caprilli E., Della Ventura G., Williams T.C., Parodi G.C., Tuccimei P., 2006. The crystal chemistry of non-metamict pyrochlore-group minerals from Latium, Italy. *The Canadian Mineralogist* 44, 1367-1378.
- Chakhmouradian A., Williams C., 2004. Mineralogy of high-field-strength elements (Ti, Nb, Zr, Ta, Hf) in phoscoritic and carbonatitic rocks of the Kola Peninsula, Russia. In: Wall, F., Zaitsev, A. (Eds.): *Phoscorites and carbonatites from mantle to mine: the key example of the Kola Alkaline Province*. Mineralogical Society of London, 293-340.
- Chakhmouradian A.R., Reguir E.P., Kressall R.D., Crozier J., Pisiak L.K., Sidhu R., Yang P., 2015. Carbonatite-hosted niobium deposit at Aley, northern British Columbia (Canada): Mineralogy, geochemistry and petrogenesis. *Ore Geology Reviews* 64, 642-666.
- Chebotaev D.A., Doroshkevich A., Klemd R., Karmanov N., 2017. Evolution of Nb-mineralization in the Chuktukon carbonatite massif, Chadobets upland (Krasnoyarsk Territory, Russia). *Periodico di Mineralogia* 86, 99-118.
- Cordeiro P.F.O., Brod J.A., Palmieri M., de Oliveira C.G., Barbosa E.S.R., Santos R.V., Gaspar J.C., Assis L.C., 2011. The Catalão I niobium deposit, central Brazil: Resources, geology and pyrochlore chemistry. *Ore Geology Reviews* 41, 112-121.
- Harlov D.E. and Förster H.-J., 2003. Fluid-induced nucleation of (Y+REE)-phosphate minerals within apatite: Nature and experiment. Part II. Fluorapatite. *American mineralogist* 88, 1209-1229.
- Harlov D.E., Wirth R., Förster H.-J., 2005. An experimental study of dissolution-reprecipitation in fluorapatite: fluid infiltration and the formation of monazite. *Contributions to Mineralogy and Petrology* 150, 268-286.
- Hogarth D., 1977. Classification and nomenclature of the pyrochlore group. *American mineralogist* 62, 403-410.
- Hogarth D., Williams C., Jones P., 2000. Primary zoning in pyrochlore group minerals from carbonatites. *Mineralogical Magazine* 64, 683-697.
- Jan M.Q., Kamal M., Qureshi A.A., 1981. Petrography of Shilman carbonatite complex, Khyber Agency. *Geological Bulletin, University of Peshawar* 17, 61-68.
- Kempe D.R. and Jan M.Q., 1970. An alkaline igneous province in the North-West Frontier province, West Pakistan. *Geological Magazine* 107, 395-398.
- Kempe D.R.C. and Jan M.Q., 1980. The Peshawar Plain Alkaline Igneous Province, NW Pakistan. *Geological Bulletin, University of Peshawar* 13, 71-77.
- Khan A., 2021. Petrochronology, Geochemistry and Rare Earth Element Potential of Himalayan Carbonatite Complexes, Northwest Pakistan. PhD Thesis, University of Peshawar, 177 pp.
- Khattak N.U., Akram M., Khan M.A., Khan H.A., 2008.

- Emplacement time of the Loe–Shilman carbonatite from NW Pakistan: Constraints from fission-track dating. *Radiation Measurements* 43, S313-S318.
- Khromova E., Doroshkevich A., Sharygin V., Izbrodin L., 2017. Compositional evolution of pyrochlore-group minerals in carbonatites of the Belaya Zima Pluton, Eastern Sayan. *Geology of Ore Deposits* 59, 752-764.
- Knudsen C., 1989. Pyrochlore group minerals from the Qaqarssuk carbonatite complex. In: Möller, P., Cerný, P., Saupé, F. (Eds.): *Lanthanides, tantalum and niobium*. Springer, 80-99.
- Le Bas M., Mian I., Rex D., 1987. Age and nature of carbonatite emplacement in North Pakistan. *Geologische Rundschau* 76, 317-323.
- Lee M.J., Lee J.I., Garcia D., Moutte J., Williams C.T., Wall F., Kim Y., 2006. Pyrochlore chemistry from the Sokli phoscorite-carbonatite complex, Finland: implications for the genesis of phoscorite and carbonatite association. *Geochemical Journal* 40, 1-13.
- Lumpkin G.R. and Ewing R.C., 1995. Geochemical alteration of pyrochlore group minerals: pyrochlore subgroup. *American mineralogist* 80, 732-743.
- Mitchell R.H., Wahl R., Cohen A., 2020. Mineralogy and genesis of pyrochlore apatite from The Good Hope Carbonatite, Ontario: A potential niobium deposit. *Mineralogical Magazine* 84, 81-91.
- Nasraoui M. and Bilal E., 2000. Pyrochlores from the Lueshe carbonatite complex (Democratic Republic of Congo): a geochemical record of different alteration stages. *Journal of Asian Earth Sciences* 18, 237-251.
- Paton C., Hellstrom J., Paul B., Woodhead J., Hergt J., 2011. Iolite: Freeware for the visualisation and processing of mass spectrometric data. *Journal of Analytical Atomic Spectrometry* 26, 2508-2518.
- Wall F., Williams C., Woolley A., Nasraoui M., 1996. Pyrochlore from weathered carbonatite at Lueshe, Zaire. *Mineralogical Magazine* 60 (402), 731-750.
- Walter B., Parsapoor A., Braunger S., Marks M., Wenzel T., Martin M., Markl G., 2018. Pyrochlore as a monitor for magmatic and hydrothermal processes in carbonatites from the Kaiserstuhl volcanic complex (SW Germany). *Chemical Geology* 498, 1-16.
- Williams C., Wall F., Woolley A., Phillip S., 1997. Compositional variation in pyrochlore from the Bingo carbonatite, Zaire. *Journal of African Earth Sciences* 25, 137-145.
- Zirner A.L., Marks M.A., Wenzel T., Jacob D.E., Markl G., 2015. Rare earth elements in apatite as a monitor of magmatic and metasomatic processes: The Ilimaussaq complex, South Greenland. *Lithos* 228, 12-22.
- Zurevinski S.E. and Mitchell R.H., 2004. Extreme compositional variation of pyrochlore-group minerals at the Oka carbonatite complex, Quebec: evidence of magma mixing? *The Canadian Mineralogist* 42, 1159-1168.



This work is licensed under a Creative Commons Attribution 4.0 International License CC BY. To view a copy of this license, visit <http://creativecommons.org/licenses/by/4.0/>

